Chemistry Europe
European Chemical Societies Publishing

WILEY VCH

Excellence in Chemistry Research

Announcing our new flagship journal

- Gold Open Access
- Publishing charges waived
- Preprints welcome
- Edited by active scientists

Meet the Editors of *ChemistryEurope*

Luisa De Cola
Università degli Studi di Milano Statale, Italy

Ive Hermans
University of Wisconsin-Madison, USA

Ken Tanaka
Tokyo Institute of Technology, Japan

Chemistry–A European Journal
Research Article
doi.org/10.1002/chem.202203250
Chemistry Europe
European Chemical Societies Publishing
www.chemeurj.org

Check for updates

G-Quadruplex Binding of an NIR Emitting Osmium Polypyridyl Probe Revealed by Solution NMR and Time-Resolved Infrared Studies

Kateřina Peterková[+],[a, b, c] Mark Stitch[+],[d] Rayhaan Z. Boota,[e] Paul A. Scattergood,[e] Paul I. P. Elliott,[e] Michael Towrie,[f] Peter Podbevšek,[a] Janez Plavec,*[a, c, g] and Susan J. Quinn*[d]

Abstract: G-quadruplexes are emerging targets in cancer research and understanding how diagnostic probes bind to DNA G-quadruplexes in solution is critical to the development of new molecular tools. In this study the binding of an enantiopure NIR emitting $[Os(TAP)_2(dppz)]^{2+}$ complex to different G-quadruplex structures formed by human telomer (hTel) and cMYC sequences in solution is reported. The combination of NMR and time-resolved infrared spectroscopic techniques reveals the sensitivity of the emission response to subtle changes in the binding environment of the complex. Similar behaviour is also observed for the related complex $[Os(TAP)_2(dppp2)]^{2+}$ upon quadruplex binding.

Introduction

Guanine quadruplexes (G4) are important therapeutic targets whose structures have been visualized in living cells and their role in biological processes is becoming increasingly apparent.[1] Significantly, G4 sequences are found in human telomeres (hTel) and are overrepresented in the promoter regions of oncogenes.[2] Anticancer drugs that target G4 s are being actively pursued in a number of clinical trials.[2a,3] It is estimated that there are over 700,000 putative G4 forming sequences in the human genome.[4] Understanding the biological role of these structures requires the availability of molecular tools such as small luminescent probes to track and detect the structures in vitro and in vivo[5] or agents that encourage G4 formation and extraction for sequencing analysis.[6] Transition metal polypyridyl complexes are excellent candidates for these tasks as their optical and structural properties, as well as their DNA binding affinity, can be readily tuned by altering the polypyridyl ligands and metal centre.[7] To date, Ru(II)polypyridyl complexes have shown promise as G4 probes due to their tunable photophysical and structural properties. A number of dinuclear complexes have also been found to bind to G4 structures.[8],[9] While mononuclear systems have been shown to bind to cellular G4 structures,[10] where they can act to inhibit telomerase,[11] trigger apoptosis in cancer cells through G4 stabilization,[12] and to sensitize photoreactions with G4 s.[13] A recent exciting study has reported enantiospecific hTel G4 binding leading to strong inhibition of replication.[14] Osmium (II) complexes have the potential to expand this further, as in addition to their structural versatility and photostability, they typically display panchromatic absorption and extended emission in the NIR,[15] and can also act as transmission electron microscopy (TEM)[15g] and stimulated emission depletion (STED) imaging agents.[15h]

While X-ray crystallography provides definitive visualization of binding modes to DNA, finding conditions to yield good

[a] *K. Peterková,[+] Dr. P. Podbevšek, Prof. J. Plavec*
Slovenian NMR Center
National Institute of Chemistry
Hajdrihova 19, 1000, Ljubljana (Slovenia)
E-mail: janez.plavec@ki.si

[b] *K. Peterková[+]*
National Centre for Biomolecular Research
Faculty of Science, Masaryk University
Kamenice 5, 62500 Brno (Czechia)

[c] *K. Peterková,[+] Prof. J. Plavec*
Faculty of Chemistry and Chemical Technology
University of Ljubljana
Večna pot 113, 1000 Ljubljana (Slovenia)

[d] *M. Stitch,[+] Dr. S. J. Quinn*
School of Chemistry
University College Dublin
Dublin 4 (Ireland)
E-mail: susan.quinn@ucd.ie

[e] *R. Z. Boota, Dr. P. A. Scattergood, Prof. P. I. P. Elliott*
Department of Chemical Sciences
School of Applied Sciences University of Huddersfield
Queensgate, Huddersfield, HD1 3DH (UK)

[f] *Prof. M. Towrie*
Rutherford Appleton Laboratory, STFC
Harwell Campus, OX11 0FA (UK)

[g] *Prof. J. Plavec*
EN-FIST Centre of Excellence
Trg OF 13, 1000 Ljubljana (Slovenia)

[+] *These two authors contributed equally to this manuscript*

Supporting information for this article is available on the WWW under https://doi.org/10.1002/chem.202203250

© 2022 The Authors. Chemistry - A European Journal published by Wiley-VCH GmbH. This is an open access article under the terms of the Creative Commons Attribution License, which permits use, distribution and reproduction in any medium, provided the original work is properly cited.

© 2022 The Authors. Chemistry - A European Journal published by Wiley-VCH GmbH

15213765, 2023, 11, Downloaded from https://chemistry-europe.onlinelibrary.wiley.com/doi/10.1002/chem.202203250 by Kemijski Institut, Wiley Online Library on [22/02/2023]. See the Terms and Conditions (https://onlinelibrary.wiley.com/terms-and-conditions) on Wiley Online Library for rules of use; OA articles are governed by the applicable Creative Commons License

quality crystals can present a significant barrier, especially for unimolecular G4 s.[16] Indeed, crystallization of a transition metal polypyridyl complex bound to a naturally occurring unimolecular G4 sequence is yet to be reported, but a nice recent study has obtained a structure with the modified human telomer sequence.[14] X-ray crystallography also captures one single binding configuration when others may be sampled in solution and cannot always be used to study G4 s under the conditions that mimics their physiological environment. For these reasons, NMR structural studies continue to be critical to the study of G4 binding interactions,[16] extending to monitoring interactions in cells.[17] An exemplar NMR study by the Thomas group revealed the sensitivity of binding to the presence of phen or bpy ancillary ligands in a dinuclear ruthenium complex bound to the hTel structure.[9b] We have also shown how time-resolved infrared (TRIR) spectroscopy is a powerful technique for the study of DNA binding interactions.[18] This is because it can be used to exclusively monitor the DNA bases in the binding site due to their response to the formation of an excited state of the bound complex formed by visible light excitation. This phenomenon can be considered as a 'Stark-like' effect associated with the sensitivity of the ground state vibrations of the nucleobases to the redistribution of electron density in the excited state. We have recently used this technique to report on the binding interactions of the $[Ru(phen)_2(dppz)]^{2+}$ (dppz = dipyrido[3,2-a:2′,3′-c]phenazine) light switch complex with the cytosine dimers in the i-motif structure[18b] and also the G4 quartets and loop regions of different topologies of the hTel sequence.[18c]

In the current study, we show the importance of combining structural and photophysical studies, to resolve the impact of G4 binding on the luminescence response of the enantiomers of the osmium tetraazaphenanthrene (TAP) probe $[Os(TAP)_2(dppz)]^{2+}$ (**1**) and the isostructural $[Os(TAP)_2(dppp2)]^{2+}$ (dppp2 = pyrido[2′,3′:5,6]pyrazino[2,3-*f*][1,10]phenanthroline) (**2**), see Figure 1. We have recently reported that both **1** and **2** show enhanced luminescence in the presence of double stranded DNA and that subtle changes to the intercalating ligand, dppz versus dppp2, modulates the enhancement response to AT compared to GC DNA.[19] Notably, the extended dppz ligand is capable of forming favourable stacking interactions with G4 structures.[18c] This ability to stack with guanine quartets was investigated for two different G4 structures (i) the parallel-type structure, formed by a sequence derived from the cMYC promoter and (ii) the hybrid-type formed by the hTel sequence. The hybrid-1 topology of hTel features G-tracts connected by one propeller and two edgewise loops, which can obstruct the potential interaction of G-quartets with a ligand. On the other hand, parallel cMYC G4 contains only propeller loops making its G-quartets fully available for the stacking interactions with a dppz complex (Figure 1). Selective binding to G4 structures is a challenging goal. However, access to the different enantiomeric structures of polypyridyl metal complexes offers the possibility to discriminate between different looped arrangements. In particular, the influence of subtle differences in the binding environment on the access to protection from solvent molecules or dissolved oxygen, which is known to impact the emission of these complexes. We were interested to examine the binding of the delta and lambda enantiomers of **1** to these structures and the impact on the NIR emission and to explore whether this is also the case for the closely related complex **2**.

Results

Complex **1** displays weak phosphorescence at 750 nm in aqueous solution.[19] This emission is found to be enhanced in the presence of increasing concentrations of both hTel and cMYC G4 structures, which is accompanied by modest changes in the visible absorption spectrum associated with the MLCT transition (Figures 2 and S1-S2). Note the G4 solution structures were confirmed in advance of the titration by circular dichroism (Figure S3). The enhancement (I_{G4}/I_o) in de-aerated solution is more pronounced for the cMYC G4 structure, which also shows enantiomeric related enhancement of Λ-**1** (4.4x) compared to Δ-**1** (2.2x) (Figures 2 and S1). In contrast, the hTel structure exhibited less enhancement and less enantiomeric preference Λ-**1** (2.2x) versus Δ-**1** (1.7x). The changes in the emission

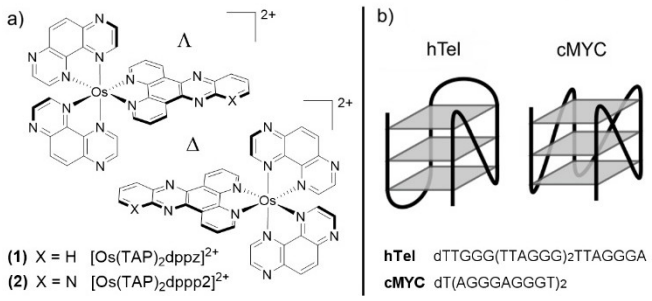

Figure 1. (a) Structures of Λ and Δ enantiomers of complexes **1** and **2**, TAP = 1,4,5,8-tetraazaphenanthrene. dppz = dipyrido[3,2-a:2′,3′-c]phenazine; dppp2 = pyrido[2′,3′:5,6]pyrazino[2,3-f][1,10]phenanthroline and (b) schematic representation of G4 structures.

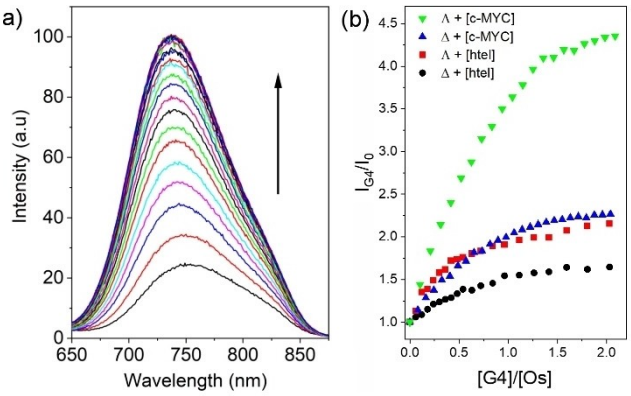

Figure 2. (a) (b) Change in the emission at 750 nm for enantiomers of **1** (ca 10 μM) in the presence of increasing [G4] recorded in 20 mM potassium phosphate buffer containing 70 mM KCl solution. I_{G4} = emission in the presence of G4 and I_o = emission in buffer. λ_{exc} = 465 nm.

© 2022 The Authors. Chemistry - A European Journal published by Wiley-VCH GmbH

15213765, 2023, 11, Downloaded from https://chemistry-europe.onlinelibrary.wiley.com/doi/10.1002/chem.202203250 by Kemijski Institut, Wiley Online Library on [22/02/2023]. See the Terms and Conditions (https://onlinelibrary.wiley.com/terms-and-conditions) on Wiley Online Library for rules of use; OA articles are governed by the applicable Creative Commons License

intensity were used to determine the binding affinity using the Bard binding model,[20] which were found to be of the order of 10^5 to 10^6 M^{-1} (Table 1). To investigate the origins of the different luminescence response, NMR and time-resolved infrared (TRIR) measurements were performed.

The ^{1}H NMR spectrum of cMYC alone was in agreement with the formation of a previously reported G4 structure consisting of three G-quartets (PDB ID: 2LBY[21]) (Figure S4). Upon titration of the DNA solution with 0.5 molar equivalents of Λ-**1**, the methyl resonance of T1 and imino resonances of G3, G7, G12 and to a lesser extent G8 were found to broaden and shift upfield (Figures 3a and S5a). These resonances continued to broaden and shift as the concentration of Λ-**1** increased up to 2 molar equivalents. Only minor chemical shift changes and line-broadening were observed for all other residues. Some imino resonances could not be traced unambiguously during the titration experiments due to spectral overlap. Importantly, no new resonances were observed during titration experiments thus excluding any global structural change of the cMYC G4 upon interaction with Λ-**1**. Our data suggests that the main interaction site of Λ-**1** is the 5′-quartet. Interestingly, as Λ-**1** was titrated into the DNA solution, ligand resonances were broadened to baseline, even when the complex was present in excess at 2 molar equivalents. The pronounced broadening of Λ-**1** resonances suggests that its binding to the G4 structures is in the intermediate exchange regime on the NMR timescale.

In order to identify how Λ-**1** interacts with the cMYC G4 structure, we performed a "reversed" titration experiment, where we added from 0.05 to 1 molar equivalent of cMYC DNA into a solution of Λ-**1** at identical salt concentration and pH. ^{1}H resonances of free Λ-**1** were assigned on the basis of ROESY spectra (Figure S6, Table S1) and previously reported assignment of $[Ru(TAP)_2(dppz)]^{2+}$.[22] Upon addition of 0.05 molar equivalents of cMYC DNA, resonances of A, B, C and D protons corresponding to the dppz part of Λ-**1** became significantly broader and shifted upfield (Figure 3e). Further broadening was observed as the DNA concentration increased. Based on selective broadening of resonances we can conclude that interaction with cMYC DNA occurs mainly via the dppz part of Λ-**1**. The Δ-**1** enantiomer showed similar DNA binding properties as Λ-**1** when titrated into a solution of cMYC DNA. Imino resonances of G3, G7, G8, G12 and methyl resonance of T1 were the most affected by complex binding (Figures 3b and S5b). The trend of line-broadening and upfield chemical shift changes of specific resonances continued with increasing concentration of **1**. The ligand resonances were broadened to baseline at 0.5

Table 1. DNA binding constants determined for **1** with cMYC and hTel DNA, using the Bard[20] treatment of luminescence band at 750 nm.

System	Binding Constant	Binding site size (per G-quartet)
Δ-**1** and [c MYC]	5.0 (±0.3)×10^5 M^{-1} 5(40%)	1.2 (±0.1)
Λ-**1** and [cMYC]	1.0 (±0.2)×10^6 M^{-1}	1.1 (±0.1)
Δ-**1** and [hTel]	3.2 (±0.8)×10^5 M^{-1}	1.0 (±0.1)
Λ-**1** and [hTel]	4.0 (±0.8)×10^5 M^{-1}	2.1 (±0.2)

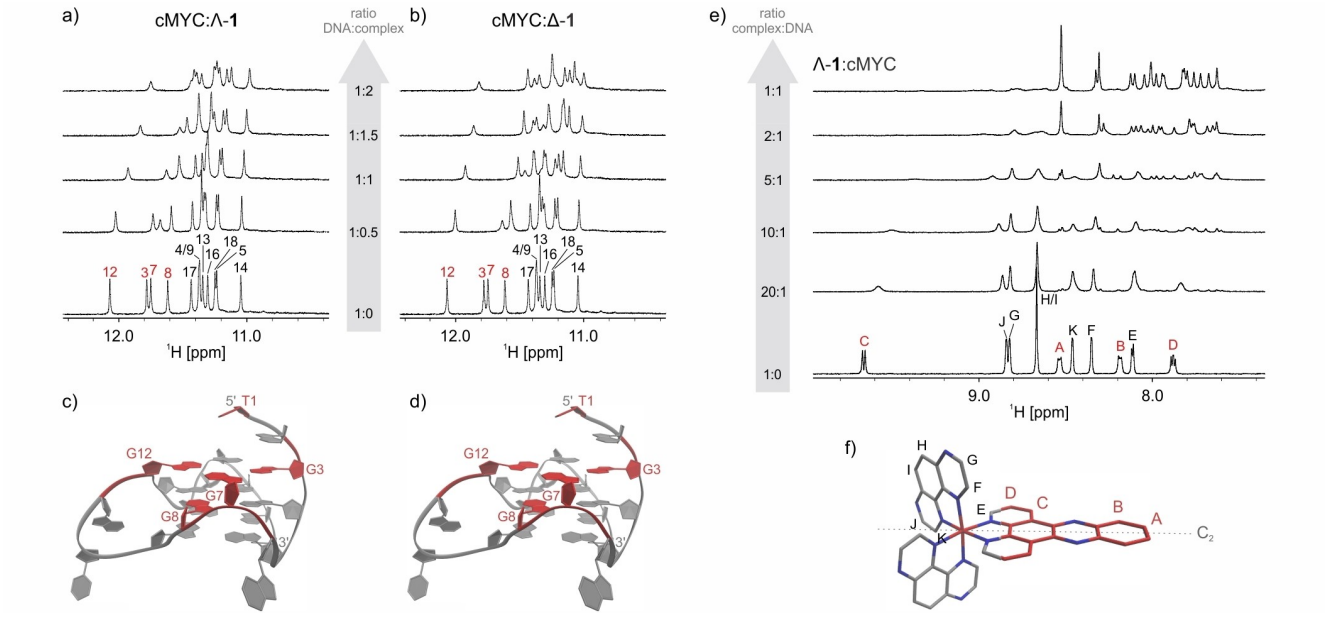

Figure 3. Imino regions of 1D ^{1}H NMR spectra of the cMYC G4, d(TAGGGAGGGTAGGGAGGGT), with increasing (a) [Λ-**1**] and (b) [Δ-**1**] from 0 to 2.0 molar equivalents. Mapping of changes in 1D ^{1}H NMR spectra upon addition of (c) Λ-**1** and (d) Δ-**1** on the solution NMR structure of cMYC (PDB: 2LBY)[15]. Nucleotides relevant for complex binding are highlighted in red. (e) Aromatic regions of 1D ^{1}H NMR spectra of Λ-**1** with increasing [cMYC]. Mapping of changes in 1D ^{1}H NMR spectra upon addition of cMYC G4 on the structure of Λ-**1**. (f) Λ-**1**. Part of the ligand relevant for binding is highlighted in red. Spectra were recorded on a 600 MHz NMR spectrometer with 70 mM KCl, 25 mM K-phosphate buffer, pH 7, 298 K, in 90% H_2O and 10% D_2O.

© 2022 The Authors. Chemistry - A European Journal published by Wiley-VCH GmbH

15213765, 2023, 11, Downloaded from https://chemistry-europe.onlinelibrary.wiley.com/doi/10.1002/chem.202203250 by Kemijski Institut, Wiley Online Library on [22/02/2023]. See the Terms and Conditions (https://onlinelibrary.wiley.com/terms-and-conditions) on Wiley Online Library for rules of use; OA articles are governed by the applicable Creative Commons License

molar equivalents of Δ-**1** and higher (Figure S7). Similarly, to Λ-**1**, interaction between cMYC and Δ-**1** occurs between the dppz part of Δ-**1** and the 5′-quartet of cMYC G4 (Figure 3c-d). While both Λ-**1** and Δ-**1** interact with cMYC G4 via its 5′-quartet, binding of the two enantiomers resulted in subtle differences in chemical shifts and line widths of imino and methyl resonances at equivalent [Complex]:[DNA] molar ratios. Due to the different ancillary ligand orientation, positioning of Λ-**1** and Δ-**1** on top of the 5′-quartet of cMYC cannot be identical. Even slight repositioning of (dppz) ring currents would cause changes in (de)shielding of nearby DNA ^{1}H NMR resonances, which can be observed in NMR spectra of the two enantiomers.

Next, interactions of Λ-**1** and Δ-**1** with the G4 structure of hTel were considered. The ^{1}H NMR spectrum of hTel confirmed a single G4 species is formed in solution as was shown previously (PDB ID: 2GKU[23]) (Figure S8). Surprisingly, upon the addition of 0.5 molar equivalents of Λ-**1**, all imino resonances of hTel G4, except G10 and G11, broadened substantially (Figure 4a). This broadening of the majority of hTel resonances suggests that the interaction with Λ-**1** is nonspecific. In contrast, the addition of 0.5 molar equivalents of Δ-**1** to a solution of hTel G4 resulted in line-broadening and upfield shifting of imino resonance of G21 and methyl resonances of T1, T2, T18 and T19 (Figures 4b and S9). The affected resonances were assigned to residues near the 5′-end. Our data indicates a more selective mode of binding for Δ-**1**, with interactions occurring predominantly with the 5′-quartet and adjacent loop nucleotides of hTel G4.

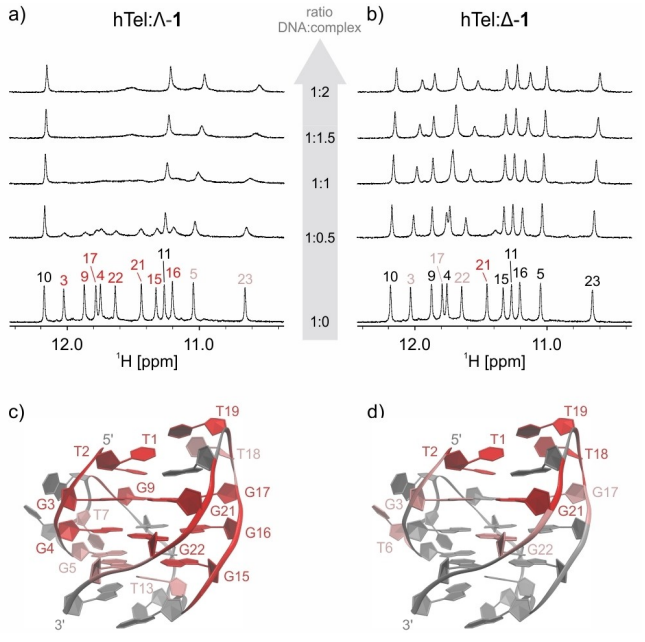

Figure 4. Imino region of 1D ^{1}H NMR spectra of hTel G4, d-(TTGGGTTAGGGTTAGGGTTAGGGA), with increasing (a) [Λ-**1**] and (b) [Δ-**1**] from 0 to 2.0 molar equivalents. Spectra were recorded on a 600 MHz NMR spectrometer with 0.1 mM DNA, 70 mM KCl, 20 mM K-phosphate buffer, pH 7, 298 K, in 90 % H_2O and 10 % D_2O. Mapping of the observed changes in 1D ^{1}H NMR spectra upon addition of (c) Λ-**1** and (d) Δ-**1** on the solution NMR structure of hTel (PDB: 2GKU).[17] Nucleotides relevant for binding are highlighted in red.

Resonances of both $[Os(TAP)_2(dppz)]^{2+}$ enantiomers were broadened to baseline when present in hTel solution at molar ratios between 0.5 and 2.0 equivalents suggesting binding in the intermediate exchange regime for **1** to hTel. Similar to the cMYC, incremental addition of hTel to a solution of Λ-**1** induced significant broadening and chemical shift changes of A, B, C and D resonances confirming that Λ-**1** interacts with hTel via the dppz ligand (Figure S10a). The same resonances were broadened during the "reversed" titration experiment with Δ-**1**, however, the broadening effect on dppz resonances was found to be much weaker compared to Λ-**1** (Figure S10b). The interaction of **1** with hTel was therefore shown to be enantioselective.

Aggregation study

Complexes containing large polyaromatic surfaces are prone to self-aggregation that occurs via π-π stacking and that can affect their binding properties. To determine whether $[Os(TAP)_2(dppz)]^{2+}$ aggregates under conditions used to evaluate G4 binding, we performed a concentration-dependent NMR study with Δ-**1**. No chemical shift changes were observed at up to 400 μM suggesting that Δ-**1** does not aggregate at the maximum concentration used for binding studies (Figures S11 and S12). However, at higher concentration of Δ-**1** (≥ 1000 μM), a broadening and slight upfield shifting of dppz ^{1}H NMR resonances were observed. This can be ascribed to formation of aggregates through π-π stacking and restriction of intramolecular motions. The same behaviour is expected for Λ-**1**.

UV melting experiments

The effect of binding of **1** on the stability of G4 structures was evaluated with a UV melting study at 295 nm as the absorption of **1** does not exhibit significant temperature-dependence at this wavelength. All melting profiles exhibit monophasic behaviour. Free cMYC and hTel G4 s exhibit melting transition ($T_{1/2}$) at 78 °C and 68 °C, respectively. Addition of 1 molar equivalent of Λ-**1** or Δ-**1** into solutions of cMYC resulted in a 2 °C increase in $T_{1/2}$ (Figure S13). Similarly, complexes of hTel with equimolar amounts of Λ-**1** or Δ-**1** resulted in a 2 and 1 °C increase in $T_{1/2}$, respectively. In contrast to melting profiles of free G4 structures, we observed a hysteresis in the melting profiles of all four complexes indicating that the structural transition is slow relative to the temperature gradient.

Time-resolved infrared experiments

The TRIR spectrum of **1**, resulting from 400 nm excitation, closely resembles that of the isostructural and extensively studied $[Ru(TAP)_2(dppz)]^{2+}$ complex (Figure S14).[18a] There is a strong transient at 1465 cm^{-1} accompanied by bleaches associated with the ground state vibrations of the polypyridyl ligands at 1496 cm^{-1}, 1529 cm^{-1}, 1581 cm^{-1} and 1620 cm^{-1}.

© 2022 The Authors. Chemistry - A European Journal published by Wiley-VCH GmbH

15213765, 2023, 11, Downloaded from https://chemistry-europe.onlinelibrary.wiley.com/doi/10.1002/chem.202203250 by Kemijski Institut, Wiley Online Library on [22/02/2023]. See the Terms and Conditions (https://onlinelibrary.wiley.com/terms-and-conditions) on Wiley Online Library for rules of use; OA articles are governed by the applicable Creative Commons License

Notably, there are no vibrations in the region of the carbonyl vibrations of guanine and thymine (ca $>1620\ cm^{-1}$).

When the TRIR measurement is repeated for either Λ-**1** or Δ-**1** excited at 400 nm in the presence of one equivalent of cMYC a new bleach band is observed at 1675 cm^{-1} (Figure 5). Critically, this strong bleach is only associated with the guanine carbonyl vibrations in the binding site and reflects a close interaction with Λ-**1** and Δ-**1**. There are no accompanying bleaches associated with the thymine bases, which supports the primary interaction with the guanine bases, and is in good agreement with the NMR assignment. The TRIR spectra recorded for Λ-**1** or Δ-**1** in the presence of hTel again shows a strong bleach associated with the guanine carbonyl at 1668 cm^{-1} (Figure S15).The intensity of the guanine bleach in the presence of hTel is found to be greater for Λ-**1**, which indicates a greater interaction under these conditions and reflects the difference in binding affinity observed in the steady state titrations. Notably, a new transient band is present at 1650 cm^{-1}, which is overlapping with the guanine bleach. For this system the role of one electron oxidation of the bases can be ruled out due to the absence of emission quenching and also the low $Os^{II/III}$ oxidation potential (+1.39 V vs. Ag/AgCl).[19] Furthermore, the 400 nm excitation cannot directly excite DNA. For these reasons the new transient is assigned to a perturbation of the thymine carbonyl ($\nu_{C4=O4}$) and guanine vibrations, which results in a shift in the absorption of the ground state vibration.

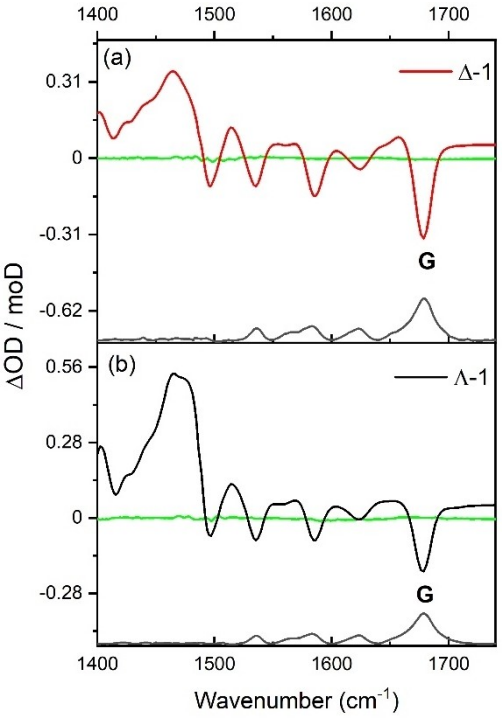

Figure 5. TRIR spectra recorded at 50 ps of 0.4 mM of 1 in the presence of 0.4 mM of cMYC in 25 mM K-phosphate and 70 mM KCl, pH 7, in D_2O (λ_{ex} = 400 nm, 2 kHz,150 fs).

Discussion

Together the solution studies provide important information about the binding environment in solution. The TRIR study selectively probes the bases in the binding site and confirms that the primary interaction occurs through binding with the guanine quartets through π-π stacking interactions. This is not found to be a highly stabilizing interaction with only a modest change in the melting temperature observed.[24,25] In the case of the cMYC structure the NMR studies indicate that the parallel topology of cMYC accommodates both Λ-**1** and Δ-**1** species at the 5′-quartet site, which is supported by the TRIR data. Notably, the NMR studies indicate a very similar binding site for Λ-**1** and Δ-**1**, but the sensitivity of the measurement to the dppz ring current reveals that the orientation/overlap of the intercalating dppz ligand differs between enantiomers. Critically, this observation suggests that a subtle change in the environment of **1** can have a significant impact on the luminescence as seen by the greater emission enhancement observed for Λ-**1** over Δ-**1** (Figure 1). In contrast, the NMR studies on the hTel G4 binding reveal increased enantioselective binding to the more compact hybrid topology. In this case, while non-specific interactions are observed for Λ-**1**, binding of Δ-**1** is found to occur at the 5′-quartet and adjacent loop nucleotides. Interestingly, the results from the emission titrations indicate that neither of these binding sites appear optimum for significant emission enhancement.

To further investigate these effects the visible absorption and emission titrations with the G4 structures were repeated for the closely related complex $[Os(TAP)_2(dppp2)]^{2+}$ **2**, Figure 1. This complex would be expected to bind in a similar fashion to the dppz complex. Notably, complex **2** possesses a well resolved π→π* ligand centred dppp2 transition at 355 nm, which allows direct reporting on the influence of the extended polypyridyl ligand on the surrounding bases in the G4 binding environment.[19] Interestingly, these measurements again suggest that the emission is very sensitive to subtilties in the particular binding interactions. This can be clearly seen by comparing the spectra obtained for Λ-**2** and Δ-**2** in the presence of excess cMYC G4 (Figure S16). While the absorption spectra for both enantiomers show significant (ca 37%) hypochromism at 355 nm (Figure S17), greater emission enhancement is observed for Λ-**2**. As was the case for complex **1** a smaller hypochromic shift is observed for both Λ-**2** and Δ-**2** in the presence of hTel and modest emission enhancement is observed (Figure S18). Overall, the spectroscopic trends observed for **2** are comparable to those observed for complex **1**.

In aqueous solution the emission of **1** and **2** is attributed to ^{3}MLCT states localised on the TAP ligands (though, computational studies indicate that additional dppz/dppp2 ^{3}MLCT and ^{3}LC states will be relatively close in energy).[18] Hydrogen bonding interactions between solvent molecules and the TAP non-coordinating nitrogen atoms are expected to impact the quantum yield and the observed emission. The changes in the emission will also be impacted by access to dissolved oxygen, which has been shown to decrease the emission intensity.[18] To appreciate why subtle changes in the binding may impact the

© 2022 The Authors. Chemistry - A European Journal published by Wiley-VCH GmbH

15213765, 2023, 11, Downloaded from https://chemistry-europe.onlinelibrary.wiley.com/doi/10.1002/chem.202203250 by Kemijski Institut, Wiley Online Library on [22/02/2023]. See the Terms and Conditions (https://onlinelibrary.wiley.com/terms-and-conditions) on Wiley Online Library for rules of use; OA articles are governed by the applicable Creative Commons License

emission we have shown a model of the possible interaction of Λ-**1** with the cMYC structure, see Figure 6. In this figure it is possible to see that both the environment of the dppz and the TAP ligands would change as the complex pivots in the structure.

Conclusion

NMR, TRIR and emission titrations were used to gain insight into the luminescence response to G4 binding of an osmium NIR emitting probe in solution. Notably, the luminescence response indicates a subtle sensitivity of the excited state to the binding environment, which would not necessarily be predicted from the structural studies alone. This demonstrates the challenge in designing transition metal polypyridyl complexes to respond to a specific DNA environment and the need to combine multiple solution-based techniques to resolve the influence of the binding environment. Future work will consider the ability to exploit the emission of structurally diverse osmium polypyridyl complexes to selectively target G4 systems.

Experimental Section

Oligonucleotide concentration was determined by measuring ultraviolet absorbance at 260 nm using the Varian CARY-100 BIO UV-VIS UV/VIS Spectrophotometer with 1.0 cm light path cells. An extinction coefficient of 201700 M^{-1} cm^{-1} for cMYC and 244300 M^{-1} cm^{-1} for hTel was calculated with the nearest neighbor method.

Dry Λ-**1** and Δ-**1** were dissolved in the solution containing 10% D_2O and 70 mM KCl, 20 mM K-phosphate buffer (pH 7.0) to final concentration of 8 mM. NMR samples with different ratios of oligonucleotide and complexwere prepared by titrating 8 mM aqueous solution of complex into aqueous solution of oligonucleotide or alternatively by titration of aqueous solution of oligonucleotide into the aqueous solution of complex. NMR samples for aggregation study were prepared by diluting 11 mM stock solution of Δ-**1** in aqueous solution containing 10% D_2O and 70 mM KCl, 25 mM K-phosphate buffer (pH 7.0) to achieve six different concentrations of Δ-**1**: 10, 50, 100, 400, 1000 and 2000 μM.

NMR data were collected on Bruker AVANCE III HD and AVANCE NEO 600 MHz NMR spectrometers equipped with cryogenic probes at 25 °C in 90% H_2O/10% D_2O. For suppression of water signals, the excitation sculpting pulse sequence element was used. NMR spectra were externally referenced to Sodium trimethylsilylpropanesulfonate (DSS). 2D NOESY spectra were acquired at mixing time 250 ms, 2D ROESY spectra at mixing time 250, 350 and 500 ms. NMR spectra were processed and analysed using TopSpin (Bruker). Resonance assignment was done with Sparky (NMRFAM) software. Samples for UV melting experiments were prepared by diluting NMR samples with a blank solution containing 70 mM KCl and 25 mM K-phosphate buffer (pH 7.0) for cMYC and 70 mM KCl and 20 mM K-phosphate buffer (pH 7.0) for hTel. UV-Vis absorption spectra were recorded on a Varian Cary 50 spectrophotometer. Steady-state luminescence spectra were recorded on a Varian Cary Eclipse. Circular dichroism measurements were recorded on a JASCO J-810 spectropolarimeter. UV melting experiments were performed on a Varian CARY 3500 UV-VIS spectrophotometer with the Cary Win UV Thermal program using 1.0 cm light path cells. Samples were heated/cooled at 0.5 °C·min^{-1} in the range of 10–95 °C and absorbance at 295 nm was measured at 0.5 °C steps. $T_{1/2}$ was determined from the first derivation of A295 vs. temperature plot. Attempts to dock Λ-**1** or Δ-**1** to structures of cMYC and hTel G4 s (PDB: 2LBY and 2GKU) with AutoDock for the complete G4 structures as well as structures without loop nucleotides or without loop nucleobases proved unsuccessful. This is probably due to the lack of a distinct binding pocket on the two G4 structures while favourable stacking interactions are not considered by simple ligand docking algorithms. Therefore a model of the possible interactions was instead generated using the reported ^{1}H NMR spectrum of cMYC (PDB ID: 2LBY)[18] along with the previously reported X-ray crystallography structure of $[Os(TAP)_2(dppz)]$[15] to illustrate the binding orientations of Λ-**1** with the cMYC structure, within the PyMOL Version 2.5.4 graphics user interface. This considered the binding orientation of Λ-**1** to coincide with the nucleotide interactions (highlighted in red) determined from the NMR study.

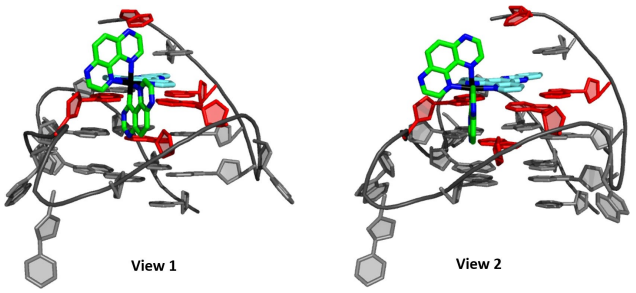

Figure 6. Structural modelling of Λ-**1** with the cMYC structure (PDB ID: 2LBY), nucleotides interaction determined from the NMR study highlighted in red, TAP ancillary ligands coloured green, dppz ligand coloured cyan and Os metal centre coloured black.

Acknowledgements

The authors would like to acknowledge the following for financial support from the European Union's Horizon 2020 research and innovation programme under the Marie Skłodowska-Curie grant agreement no 765266 (LightDyNAmics). R.Z.B. acknowledges the University of Huddersfield for the funding of a PhD studentship. K.P., P.P. and J.P. acknowledge financial support from the Slovenian Research Agency [grants P1-0242 and J1-1704]. The authors acknowledge the CERIC-ERIC Consortium for the access to experimental facilities. This project has received funding from the European Union's Horizon 2020 research and innovation programme under grant agreement no. 871124 Laserlab-Europe (Central Laser Facility, STFC ID 22130030). Open Access funding provided by IReL.

Conflict of Interest

The authors declare no conflict of interest.

© 2022 The Authors. Chemistry - A European Journal published by Wiley-VCH GmbH

15213765, 2023, 11, Downloaded from https://chemistry-europe.onlinelibrary.wiley.com/doi/10.1002/chem.202203250 by Kemijski Institut, Wiley Online Library on [22/02/2023]. See the Terms and Conditions (https://onlinelibrary.wiley.com/terms-and-conditions) on Wiley Online Library for rules of use; OA articles are governed by the applicable Creative Commons License

Data Availability Statement

The data that support the findings of this study are openly available in Zenodo at https://doi.org/10.5281/zenodo.7197136, reference number 7197136.

Keywords: G-quadruplex · luminescent enhancement · NMR · osmium polypyridyl · spectroscopy · TRIR

[1] D. Varshney, J. Spiegel, K. Zyner, D. Tannahill, S. Balasubramanian, *Nat. Rev. Mol. Cell Biol.* **2020**, *21*, 459–474.
[2] a) S. Neidle, *J. Med. Chem.* **2016**, *59*, 5987–6011; b) R. Hansel-Hertsch, D. Beraldi, S. V. Lensing, G. Marsico, K. Zyner, A. Parry, M. Di Antonio, J. Pike, H. Kimura, M. Narita, D. Tannahill, S. Balasubramanian, *Nat. Genet.* **2016**, *48*, 1267–1272.
[3] J. Carvalho, J. L. Mergny, G. F. Salgado, J. A. Queiroz, C. Cruz, *Trends Mol. Med.* **2020**, *26*, 848–861.
[4] V. S. Chambers, G. Marsico, J. M. Boutell, M. Di Antonio, G. P. Smith, S. Balasubramanian, *Nat. Biotechnol.* **2015**, *33*, 877–881.
[5] a) A. Laguerre, K. Hukezalie, P. Winckler, F. Katranji, G. Chanteloup, M. Pirrotta, J.-M. Perrier-Cornet, J. M. Y. Wong, D. Monchaud, *J. Am. Chem. Soc.* **2015**, *137*, 8521–8525; b) A. Shivalingam, M. A. Izquierdo, A. L. Marois, A. Vyšniauskas, K. Suhling, M. K. Kuimova, R. Vilar, *Nat. Commun.* **2015**, *6*, 8178; c) W.-C. Huang, T.-Y. Tseng, Y.-T. Chen, C.-C. Chang, Z.-F. Wang, C.-L. Wang, T.-N. Hsu, P.-T. Li, C.-T. Chen, J.-J. Lin, P.-J. Lou, T.-C. Chang, *Nucleic Acids Res.* **2015**, *43*, 10102–10113; d) M. Di Antonio, A. Ponjavic, A. Radzevičius, R. T. Ranasinghe, M. Catalano, X. Zhang, J. Shen, L.-M. Needham, S. F. Lee, D. Klenerman, S. Balasubramanian, *Nat. Chem.* **2020**, *12*, 832–837; e) H. Tateishi-Karimata, N. Sugimoto, *Chem. Commun.* **2020**, *56*, 2379–2390.
[6] a) F. Raguseo, S. Chowdhury, A. Minard, M. Di Antonio, *Chem. Commun.* **2020**, *56*, 1317–1324; b) S. Müller, S. Kumari, R. Rodriguez, S. Balasubramanian, *Nat. Chem.* **2010**, *2*, 1095–1098.
[7] H. K. Saeed, S. Sreedharan, J. A. Thomas, *Chem. Commun.* **2020**, *56*, 1464–1480.
[8] a) V. Gonzalez, T. Wilson, I. Kurihara, A. Imai, J. A. Thomas, J. Otsuki, *Chem. Commun.* **2008**, 1868–1870; b) S. Rickling, L. Ghisdavu, F. Pierard, P. Gerbaux, M. Surin, P. Murat, E. Defrancq, C. Moucheron, A. Kirsch-De Mesmaeker, *Chem. Eur. J.* **2010**, *16*, 3951–3961; c) L. Xu, D. Zhang, J. Huang, M. Deng, M. Zhang, X. Zhou, *Chem. Commun.* **2010**, *46*, 743–745.
[9] a) T. Wilson, M. P. Williamson, J. A. Thomas, *Org. Biomol. Chem.* **2010**, *8*, 2617–2621; b) T. Wilson, P. J. Costa, V. Felix, M. P. Williamson, J. A. Thomas, *J. Med. Chem.* **2013**, *56*, 8674–8683; c) J. Rubio-Magnieto, S. Kajouj, F. Di Meo, M. Fossepre, P. Trouillas, P. Norman, M. Linares, C. Moucheron, M. Surin, *Chem. Eur. J.* **2018**, *24*, 15577–15588.
[10] D. Sun, Y. Liu, D. Liu, R. Zhang, X. Yang, J. Liu, *Chem. Eur. J.* **2012**, *18*, 4285–4295.
[11] G. Liao, X. Chen, J. Wu, C. Qian, H. Wang, L. Ji, H. Chao, *Dalton Trans.* **2014**, *43*, 7811–7819.
[12] Z. Zhang, Q. Wu, X. H. Wu, F. Y. Sun, L. M. Chen, J. C. Chen, S. L. Yang, W. J. Mei, *Eur. J. Med. Chem.* **2014**, *80*, 316–324.
[13] J. Weynand, A. Diman, M. Abraham, L. Marcelis, H. Jamet, A. Decottignies, J. Dejeu, E. Defrancq, B. Elias, *Chem. Eur. J.* **2018**, *24*, 19216–19227.
[14] K. T. McQuaid, S. Takahashi, L. Baumgaertner, D. J. Cardin, N. G. Paterson, J. P. Hall, N. Sugimoto, C. J. Cardin, *J. Am. Chem. Soc.* **2022**, *144*, 5956–5964.
[15] a) S. Omar, P. Scattergood, L. McKenzie, H. Bryant, J. Weinstein, P. Elliott, *Molecules* **2016**, *21*, 1382; b) S. A. E. Omar, P. A. Scattergood, L. K. McKenzie, C. Jones, N. J. Patmore, A. Meijer, J. A. Weinstein, C. R. Rice, H. E. Bryant, P. I. P. Elliott, *Inorg. Chem.* **2018**, *57*, 13201–13212; c) A. Byrne, C. Dolan, R. D. Moriarty, A. Martin, U. Neugebauer, R. J. Forster, A. Davies, Y. Volkov, T. E. Keyes, *Dalton Trans.* **2015**, *44*, 14323–14332; d) K. S. Gkika, A. Byrne, T. E. Keyes, *Dalton Trans.* **2019**, *48*, 17461–17471; e) C. Ge, H. Huang, Y. Wang, H. Zhao, P. Zhang, Q. Zhang, *ACS Appl. Bio Mat.* **2018**, *1*, 1587–1593; f) K. R. A. Schneider, A. Chettri, H. D. Cole, K. Reglinski, J. Brückmann, J. A. Roque III, A. Stumper, D. Nauroozi, S. Schmid, C. B. Lagerholm, S. Rau, P. Bäuerle, C. Eggeling, C. G. Cameron, S. A. McFarland, B. Dietzek, *Chem. Eur. J.* **2020**, *26*, 14844–14851; g) A. Wragg, M. R. Gill, C. J. Hill, X. Su, A. J. Meijer, C. Smythe, J. A. Thomas, *Chem. Commun.* **2014**, *50*, 14494–14497; h) F. Dröge, F. F. Noakes, S. A. Archer, S. Sreedharan, A. Raza, C. C. Robertson, S. MacNeil, J. W. Haycock, H. Carson, A. J. H. M. Meijer, C. G. W. Smythe, J. Bernardino de la Serna, B. Dietzek-Ivanšić, J. A. Thomas, *J. Am. Chem. Soc.* **2021**, *143*, 20442–20453.
[16] A. Kellett, Z. Molphy, C. Slator, V. McKee, N. P. Farrell, *Chem. Soc. Rev.* **2019**, *48*, 971–988.
[17] G. F. Salgado, C. Cazenave, A. Kerkour, J.-L. Mergny, *Chem. Sci.* **2015**, *6*, 3314–3320.
[18] a) C. J. Cardin, J. M. Kelly, S. J. Quinn, *Chem. Sci.* **2017**, *8*, 4705–4723; b) F. R. Baptista, S. J. Devereux, S. P. Gurung, J. P. Hall, I. V. Sazanovich, M. Towrie, C. J. Cardin, J. A. Brazier, J. M. Kelly, S. J. Quinn, *Chem. Commun.* **2020**, *56*, 9703–9706; c) S. J. Devereux, F. E. Poynton, F. R. Baptista, T. Gunnlaugsson, C. J. Cardin, I. V. Sazanovich, M. Towrie, J. M. Kelly, S. J. Quinn, *Chem. Eur. J.* **2020**, *26*, 17103–17109; d) P. M. Keane, K. O'Sullivan, F. E. Poynton, B. C. Poulsen, I. V. Sazanovich, M. Towrie, C. J. Cardin, X.-Z. Sun, M. W. George, T. Gunnlaugsson, S. J. Quinn, J. M. Kelly, *Chem. Sci.* **2020**, *11*, 8600–8609; e) F. A. Baptista, D. Krizsan, M. Stitch, I. V. Sazanovich, I. P. Clark, M. Towrie, C. Long, L. Martinez-Fernandez, R. Improta, N. A. P. Kane-Maguire, J. M. Kelly, S. J. Quinn, *J. Am. Chem. Soc.* **2021**, *143*, 14766–14779.
[19] M. Stitch, R. Z. Botta, A. S. Chalkley, T. D. Keene, J. C. Simpson, P. A. Scattergood, P. I. P. Elliott, S. J. Quinn, *Inorg. Chem.* **2022**, *61*, 14947–14961.
[20] M. T. Carter, M. Rodriguez, A. J. Bard, *J. Am. Chem. Soc.* **1989**, *111*, 8901–8911.
[21] R. I. Mathad, E. Hatzakis, J. Dai, D. Yang, *Nucleic Acids Res.* **2011**, *39*, 9023–9033.
[22] I. Ortmans, B. Elias, J. M. Kelly, C. Moucheron, A. Kirsch-DeMesmaeker, *Dalton Trans.* **2004**, 668–676.
[23] K. N. Luu, A. T. Phan, V. Kuryavyi, L. Lacroix, D. J. Patel, *J. Am. Chem. Soc.* **2006**, *128*, 9963–9970.
[24] S. Shi, J.-H. Xu, X. Gao, H.-L. Huang, T.-M. Yao, *Chem. Eur. J.* **2015**, *21*, 11435–11445.
[25] E. Wachter, D. Moya, S. Parkin, E. C. Glazer, *Chem. Eur. J.* **2016**, *22*, 550–559.

Manuscript received: October 18, 2022
Accepted manuscript online: November 18, 2022
Version of record online: January 12, 2023

© 2022 The Authors. Chemistry - A European Journal published by Wiley-VCH GmbH

15213765, 2023, 11, Downloaded from https://chemistry-europe.onlinelibrary.wiley.com/doi/10.1002/chem.202203250 by Kemijski Institut, Wiley Online Library on [22/02/2023]. See the Terms and Conditions (https://onlinelibrary.wiley.com/terms-and-conditions) on Wiley Online Library for rules of use; OA articles are governed by the applicable Creative Commons License